Modeling of short geothermal boreholes in series with experimental validation

Michel Bernier, Professor, Département de génie mécanique, Polytechnique Montréal, Montréal, Québec, Canada
Odile Cauret, Researcher, Énergie dans les Bâtiments et Territoires, EDF Recherche et Développement, Moret-sur-Loing, France

Abstract:

Bore fields composed of short boreholes offer several modeling challenges. For example, ground temperatures variations in the first few meters below the ground surface are larger than the ones experienced by deep boreholes. Also, boreholes need to be piped in series to maintain a relatively high flow rate which implies that the inlet temperature to each borehole changes from one borehole to the next.

In the first part of this study a methodology to model short boreholes is proposed. First, a detailed single borehole model which includes borehole thermal capacity is introduced. Then, the entire bore field is modeled using analytical solutions to ground heat transfer and spatial and temporal superposition to predict the outlet fluid temperature from each borehole at each time step. Finally, the model is validated against experimental data obtained on a test facility composed of 16 short boreholes (9 m deep), with 4 rows of 4 boreholes in series. It is shown that the results from the proposed model are in close agreement with the experimental results if the ground temperature variation with depth is taken into account.

Key Words: borehole, ground-source heat pump

1 INTRODUCTION

Short boreholes used in ground-source heat pump (GSHP) systems have the potential of reducing capital cost often associated with deep boreholes (Cauret and Bernier, 2009; Cimmino et al., 2013). More compact drill rigs that are easier to manage and cheaper to operate can be used. However, more boreholes are required because of the reduced borehole heat transfer area. Short boreholes need to be carefully studied in order to be correctly sized and implemented as some parameters have a much greater impact on short boreholes behavior than on deep boreholes. The main parameters to investigate are the large swings in ground temperature near the surface and the thermal interferences among boreholes. In addition, contrary to traditional bore fields with boreholes in parallel, short boreholes have to be piped in series and each borehole has a different inlet temperature and consequently a different heat transfer rate.

This study proposes a model to evaluate the performance of a bore field composed of short boreholes. An experimental facility with 16 boreholes (4 rows of 4 boreholes in series) is used to validate the proposed model.

2 DESCRIPTION OF THE EXPERIMENTAL FACILITY

2.1 EDF R&D Field Test Platform

The EDF R&D field test platform is located in Moret-sur-Loing near Fontainebleau in France. It is designed to test GSHP in a natural climate over one or more years. It consists of a 3000 m^2 land area dedicated to the installation of ground collectors and a control room equipped with several heat pumps. This facility is used to experimentally check ground collector sizing, evaluate the impact of ground heat exchangers on the surrounding ground, and measure ground heat exchanger performance as well as heat pump performance. As shown in Figure 1, the set-up consists of a water-to-water heat pump connected to the ground heat exchangers. The operation of the heat pump uses a control loop which mimics the operation of a real house, with adjustable insulating level and house size and is driven by real-time weather. Thus, whenever house heating is required the heat pump is activated to heat a 500 liter tank which acts as a house. The house load is rejected outside using an air cooler loop. The control strategy reproduces the real-life operation of a house/heat pump combination.

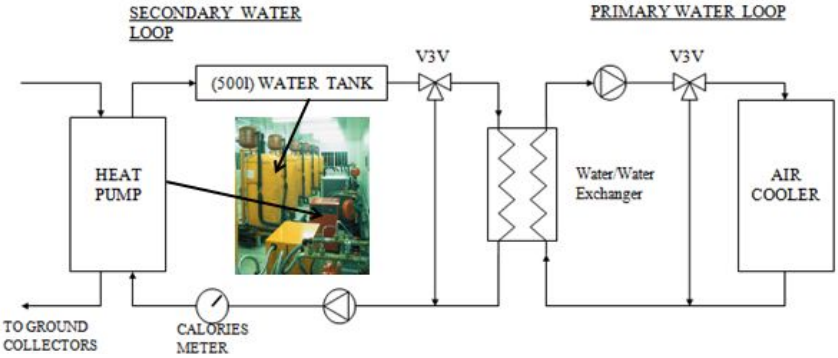

Figure 1: Schematic representation of the EDF R&D field test platform

The platform is equipped to measure the following parameters with a one-minute time step:

- thermal energy supplied to the air cooler loop
- water flow rate and temperatures (inlet/outlet) at the evacuation exchanger
- absorbed electrical energy (compressor and circulating pumps)
- brine and water temperatures (inlet/outlet) at the evaporator and condenser of the heat pump; brine flow rate at the evaporator
- outside air temperature and humidity

In addition to these measurements, which are mostly performed indoors in the control room, a number of measurements are made in the field as described below.

2.2 Short geothermal boreholes installation

The short borehole field under investigation is shown in Figure 2a and is described in detail by Rancourt-Ouimet (2012). It consists of 16 equally-spaced boreholes in a square configuration with 4 rows of 4 boreholes in series. Rows are piped to be in a counter-current flow configuration. Each borehole consists of a single U-tube and is filled with a high conductivity grout. The borehole characteristics are given in Table 1. The first row is the one closest to the manifold well and boreholes are numbered from 1 to 16 with the following sequence: borehole number #1 is the one located on the top left corner and borehole #5 is below borehole #1 and so on. With a nominal flow rate of 0.055 kg/s per row, it takes 8 minutes for the fluid to travel the distance from the inlet to the outlet of a row (i.e. 83 m as shown in Figure 2b).

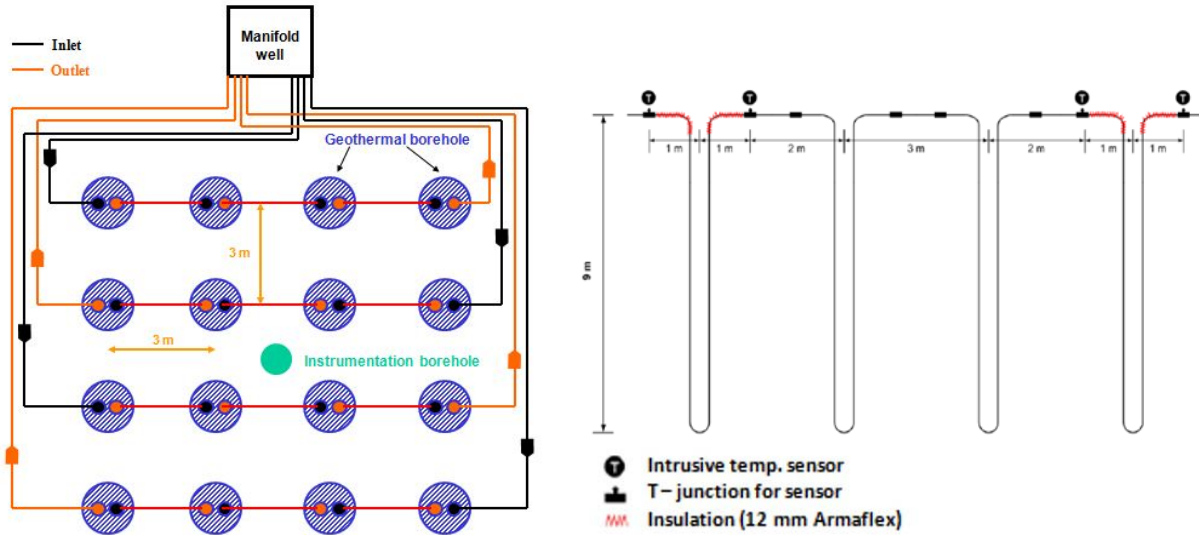

Figure 2: a) Short borehole test facility b) Cross-section showing the first row

Table 1: Bore field characteristics

Parameter	Value	Units
Borehole length	9	m
Borehole diameter	14	cm
Buried depth	1	m
Center-to-center boreholes spacing	3	m
Ground thermal conductivity	2.52	$W\text{-}m^{-1}\text{-}K^{-1}$
Ground thermal capacitance	2600	$kJ\text{-}m^{-3}\text{-}K^{-1}$
Pipe inner radius	0.0102	m
Pipe outer radius	0.013	m
Pipe thermal conductivity	0.4	$W\text{-}m^{-1}\text{-}K^{-1}$
Center-to-center pipe distance	0.045	m
Grout thermal conductivity	2	$W\text{-}m^{-1}\text{-}K^{-1}$
Grout thermal capacitance	3900	$kJ\text{-}m^{-3}\text{-}K^{-1}$
Fluid (Monopropylene glycol) concentration	30	%
Fluid density	1028	kg/m^3
Fluid specific heat	3905	$J\text{-}kg^{-1}\text{-}K^{-1}$
Fluid thermal conductivity	0.44	$W\text{-}m^{-1}\text{-}K^{-1}$
nominal flow rate per row	0.055	kg/s

2.3 Borehole temperature measurements

A number of temperature sensors are installed in the field. All temperatures are measured using 4-wires PT100 sensors. Each sensor is equipped with a second set of 4-wires for redundancy. The uncertainty associated with the temperature measurements is estimated to be ± 0.2°C.

2.3.1 Fluid temperature measurements

A total of ten intrusive temperature sensors were installed to measure the evolution of the fluid temperature in the field. Figure 2b shows the location of the four measurements in the first row which are located at the inlet and outlet of the first and fourth boreholes. For the other three rows, temperatures are measured at the inlet of the first borehole and at the outlet of the last borehole.

2.3.2 Underground temperature measurements

In the first and fourth boreholes of the first row, pipe wall temperatures are measured. The locations are shown in Figure 3a. As shown in Figure 2a, four temperature sensors have been introduced in an instrumentation borehole in the center of the field. The sensor positions are shown on Figure 3b. They are used to measure the evolution of the ground temperature at various depths.

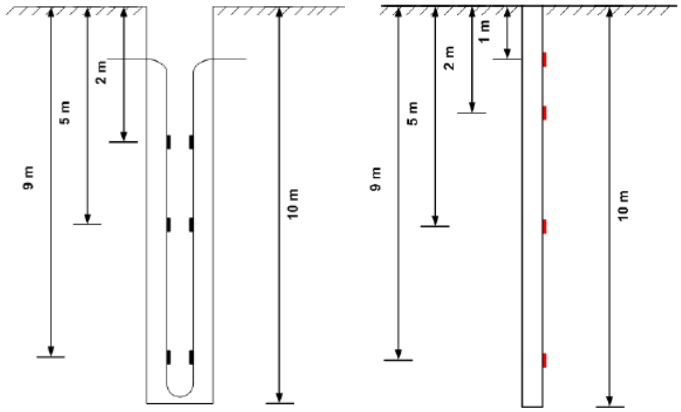

Figure 3: Temperature measurement locations. a) On the pipe wall of the first and fourth boreholes of the first row; b) Instrumentation borehole in the middle of the bore field.

Figure 4 shows the measured temperatures in the instrumentation borehole over the first heating season from November 10th, 2011 to the end of April 2012. As shown in this figure, the time variation of ground temperature with depth is significant. For example, the difference in the ground temperature at a depth of 1 and 9 m can reach 8°C around February 20th. This figure shows that there is a need to account for the ground temperature variation with depth if short boreholes are to be modeled properly.

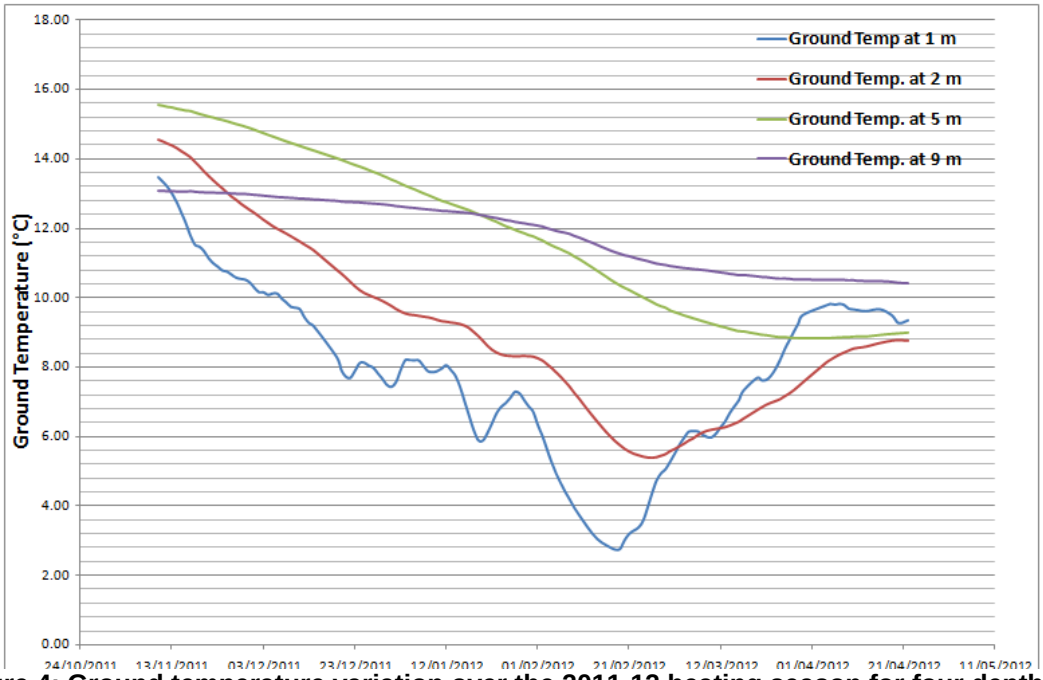

Figure 4: Ground temperature variation over the 2011-12 heating season for four depths

3 MODEL DEVELOPMENT

Two types of models are developed in the present study. First, a detailed model of a single borehole is presented. The borehole is divided in layers in the axial direction and each of these layers has a different far-field ground temperature. Radial heat transfer in the ground is calculated using the cylindrical heat source (CHS) analytical solution. The fluid and grout thermal capacities are also taken into account.

In the second approach, the entire bore field presented earlier is modeled. Since boreholes are in series they cannot be modeled using classical tools such as the DST model (Hellström et al., 1996) or the g-function approach (Eskilson, 1987). Instead, a new technique, based on analytical solutions to ground heat transfer, is used. For short times (< one day), when axial heat transfer effects are negligible, the CHS is used to predict borehole wall temperature. For longer times, the finite line source analytical solution to 2-D heat transfer is used. Spatial and temporal superposition is also used to predict the outlet fluid temperature from each borehole at each time step. An iterative solution is required as the thermal output of one borehole depends on the outlet temperature of the previous borehole. The borehole is divided into five axial layers with a proper account of the fluid and grout thermal capacities. At this stage in the development, the bore field model is built such that each layer has the same far-field ground temperature.

3.1 Single borehole model

The single borehole geometry being modeled is presented schematically in Figure 5a. The model divides the borehole heat exchanger into 10 layers along the borehole. The cross-sections of each layer are modeled using the so-called 'thermal resistance and capacity models' (TRCM) approach described by Godefroy and Bernier (2014) which accounts for the fluid and grout thermal capacity. The modeled TRCM network is presented schematically in Figure 5b. In the present case, 8 temperature nodes (shown as dots in Figure 5b) are used. These temperatures represent: i) the fluid temperature in the downward and upward pipes, ii) temperatures of both U-tube pipes, iii) three grout temperatures, iv) the borehole wall temperature. The original approach of Godefroy and Bernier (2014) is refined here to include 10 different far-field ground temperatures ($T_{g,i}$ in Figure 5b) for each borehole layer. The TRCM approach predicts the temperature variation inside the borehole while the CHS is used to model heat transfer from the borehole wall to the far-field.

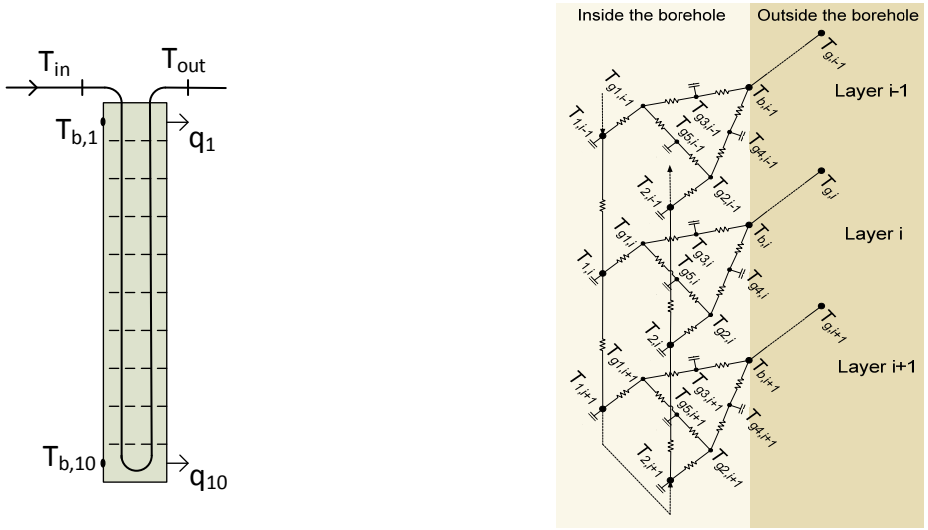

Figure 5: a) single borehole geometry ; b) TRCM representation of the borehole

3.2 Model for the entire bore field

The approach used to model the bore field depicted in Figure 2 differs somewhat from the model presented above for the single borehole as running a simulation of 16 thermally interacting boreholes with a one-minute time-step is computationally intensive. Therefore, a number of measures are taken to reduce computations. First, thermal response factors are pre-calculated using the analytical solution to the Finite Line Source (FLS) for long times (t > 1 day) and the Cylindrical Heat Source (CHS) for short times. The tabulated results are then interpolated when needed. Secondly, the TRCM approach is implemented with five axial sections, instead of 10 for the single borehole, and a single averaged far-field ground temperature is used for the entire length of the borehole. Finally, the non-insulated horizontal sections are not modeled.

3.2.1 Pre-calculated thermal response factors for a single borehole.

For the present geometry, each borehole is thermally interacting with 15 other neighboring boreholes. As shown in Figure 6a there are 10 possible distances between any borehole and its neighbors. The thermal response of a single borehole for these 10 distances are first calculated using the CHS or the FLS and then superimposed in space to account for borehole thermal interaction. Figures 6b shows a schematic of the solution of the FLS which gives a two-dimensional temperature profile (*T(r,z,t)*) at a certain radial distance *r* resulting from a heat extraction q over a period of time *t* from a finite line source of length *H* and buried at a depth *D*. Claesson and Javed (2011) proposed a relation for the integral mean temperature at the borehole wall for the case $D \geq 0$. According to the authors, the integral mean temperature at a distance *r* from the center of the borehole after a certain time *t* is given by:

$$\Delta\bar{T}(r,t) = -\frac{q}{4\pi k_s} \cdot \int_{1/\sqrt{4\alpha_s t}}^{\infty} exp(-r^2 s^2) \cdot \frac{Y(Hs,Ds)}{Hs^2} \cdot ds = -\frac{q}{4\pi k_s} \cdot TR(r,t) \quad (1)$$

$$Y(h,d) = 2 \cdot ierf(h) + 2 \cdot ierf(h+2d) - ierf(2h+2d) - ierf(2d) \quad (2)$$

$$ierf(X) = X \cdot erf(X) - \frac{1}{\sqrt{\pi}}(1 - exp(-X^2)) \quad (3)$$

where α_s is the ground thermal diffusivity, k_s is the ground thermal conductivity, q is the heat transfer per unit length of borehole (a positive value indicates heat extraction from the ground), $\Delta\bar{T} = \bar{T} - T_g$ is the average (over the length) temperature variation at a distance *r* from the center of the borehole. $\bar{T}$ is represented by a dotted line in Figure 6b.

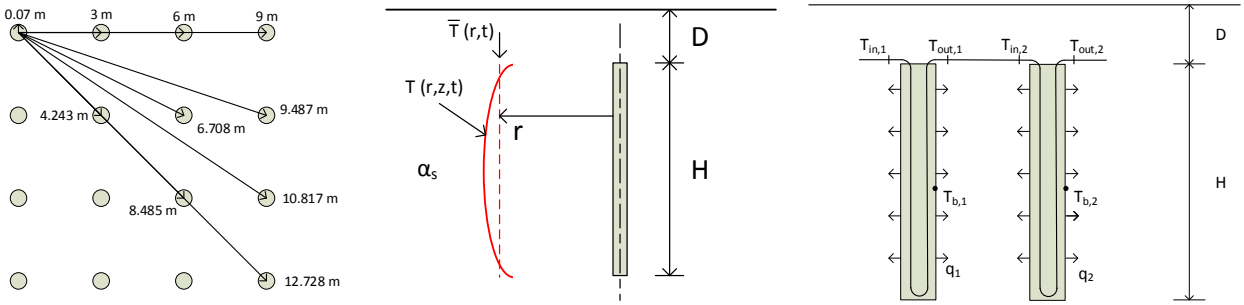

Figure 6: a) Distances between boreholes; b) Representation of the temperature profile at a distance r from a borehole; c) Series configuration

The integral in Equation 1, which will be abbreviated by the expression *TR*(*r,t*), is independent of the borehole heat transfer rate. Therefore, it can be pre-calculated for different distances and time for a given value of α_s. A partial list of results from these calculations is presented in Table 2 for α_s = 9.67×10^{-7} m^2/s (ground thermal diffusivity of the short borehole test facility). This table shows the value of the integral for times ranging from 0.432 min to 120 days for the 10 distances identified earlier. In simulations, this table is used with the value of q and k_s to determine $\Delta\overline{T}(r,t)$ using equation1. For example, for a single borehole, if the ratio $q/4\pi k_s$ is equal to 1, t = 120 days, and the far-field ground temperature is 0°C, then the average temperature (over *H*) is equal to -7.54°C at r = 0.07 m and -0.77°C at r = 3 m. Results shown in Table 2 indicate that boreholes that are far apart are not significantly affected by each other even after 120 days.

In the present approach, the FLS and the CHS are applied to only one borehole segment which covers the entire borehole length. As shown by Cimmino and Bernier (2014) it is possible to obtain more accurate thermal response factors by dividing the borehole in several segments. This approach imposes a significant computational burden and was not implemented.

Table 2: Pre-calculated thermal response factors for various times and distances from the borehole center for α_s = 9.67×10^{-7} m^2/s

1 t [days] {[min]}	2 r=.07 [m]	3 r=3 [m]	4 r=4.243 [m]	5 r=6 [m]	6 r=6.708 [m]	7 r=8.485 [m]	8 r=9 [m]	9 r=9.487 [m]	10 r=10.817 [m]	11 r=12.728 [m]
0.0003 {0.432}	0.1565	0	0	0	0	0	0	0	0	0
0.0006 {0.864}	0.2186	0	0	0	0	0	0	0	0	0
0.0009 {1.296}	0.2652	0	0	0	0	0	0	0	0	0
0.003834 {5.52}	0.5197	0	0	0	0	0	0	0	0	0
0.006 {8.64}	0.6348	0	0	0	0	0	0	0	0	0
0.01 {14.4}	0.7928	0	0	0	0	0	0	0	0	0
0.04 {57.6}	1.391	0	0	0	0	0	0	0	0	0
0.1565 {225.4}	2.247	0	0	0	0	0	0	0	0	0
0.5 {720}	3.164	0	0	0	0	0	0	0	0	0
1.2 {1728}	3.774	0	0	0	0	0	0	0	0	0
3.647 {5252}	4.818	0.00007004	0	0	0	0	0	0	0	0
31.95 {46008}	6.69	0.2363	0.06139	0.006482	0.002304	0.0001209	0.00004673	0.00001825	0.00000114	0
120 {172800}	7.539	0.7735	0.4062	0.1599	0.1079	0.03776	0.02734	0.01998	0.008121	0.001979

3.2.2 **Spatial superposition**

For the field of 16 boreholes, spatial superposition is used to obtain the temperature variation at each borehole wall:

$$\Delta T_{b,i}(t) = \bar{T}_{b,i} - T_g = \sum_{j=1}^{n_b} \Delta\bar{T}\left(d_{ij}, t\right) \qquad (4)$$

where $\Delta T_{b,i}(t)$ is the temperature variation at the wall of borehole *i*. As mentioned previously, boreholes that are far apart do not influence each other. Thus, only immediate neighbors (those that are at a distance $r \leq 4.243$ m) are considered in the summation in Equation 4. Contrary to what is usually assumed in a bore field composed of boreholes fed in parallel, each borehole as a different wall temperature in a series configuration.

3.2.3 **Series configuration**

The calculation process involved for a series configuration will be illustrated using the two boreholes shown in Figure 6c. To simplify the presentation of the equations, the heat transfer from the fluid to the borehole wall is assumed to be in steady-state and a thermal resistance, R_b, is introduced to account for this heat transfer. In the actual model, heat transfer from the fluid to the wall is accounted for using the TRCM approach as described earlier. Furthermore, a ground temperature of 0°C is assumed. The objective of the calculation is to obtain $T_{out,2}$ for known values of the inlet temperature to the first borehole, $T_{in,1}$, and of the mass flow rate, $\dot{m}$. Using spatial superposition to account for thermal interference among boreholes, the governing equations are then:

$$T_{b,1} = -\frac{q_1}{4\pi k_s} TR(0.07,t) - \frac{q_2}{4\pi k_s} TR(3,t) \quad , \quad T_{b,2} = -\frac{q_2}{4\pi k_s} TR(0.07,t) - \frac{q_1}{4\pi k_s} TR(3,t) \qquad (5)$$

$$q_1 \times H = \dot{m} Cp\left(T_{out,1} - T_{in,1}\right) \quad , \quad q_2 \times H = \dot{m} Cp\left(T_{out,2} - T_{in,2}\right) \qquad (6)$$

$$T_{b,1} - \frac{\left(T_{out,1}+T_{in,1}\right)}{2} = q_1 R_b \quad , \quad T_{b,2} - \frac{\left(T_{out,2}+T_{in,2}\right)}{2} = q_2 R_b \qquad (7)$$

A system of 6 equations and 6 unknowns is obtained and can easily be solved. A similar process is applied to the 16 boreholes to obtain the outlet temperatures at the end of each row given the inlet temperature at entrance of the row. Heat transfer rates are also superimposed in time (not shown here) using a technique described by Bernier et al. (2004).

4 RESULTS

4.1 Single borehole configuration

Simulations were performed on borehole #4 over a period of 1900 hours from the beginning of the first heating season. Thermal interaction with neighboring boreholes is considered to be negligible during this period. The single borehole TRCM model was run with the parameters presented in Table 1. The inputs to the model are the measured inlet temperature and flow rate to borehole #4. The TRCM model is used in the TRNSYS environment with a 1 min time step corresponding to the data acquisition rate of the experimental facility. Typical results for borehole #4 are shown in Figures 7 and 8 after 1531 hours of operation. Four on-off cycles are shown with an on-cycle nominal flow rate of 210 kg/h. Simulations are carried out by imposing the four measured ground temperatures as the far-field temperatures to the TRCM model (layer #1 = far-field temperature (FFT) at 1m; layers #2 and #3 = FFT at 2 m; layers #4, #5, #6, and #7 = FFT at 5m; layers #8, #9, and #10 = FFT at 9m). As shown in Figure 7, ground temperatures for these four depths are significantly different with values of 7.4°C, 9.2°C, 12.6°C, and 12.5°C at depths of 1, 2, 5, and 9 m below the surface level.

It can be seen in Figure 7 that the simulated and measured outlet temperatures are in close agreement. This is particularly true during the on-cycles where both sets of temperature are very close to each other. This indicates that the TRCM single borehole model is adequate in predicting the borehole thermal performance.

Figure 8 shows the impact of the variation of ground temperature with depth. Two on-off cycles are shown. They correspond to the second and third on-off cycles shown in Figure 7. The curves for "T_{out} measured" and for "T_{out} simulated with the ground temperature at 1, 2, 5, and 9 m" are

the same as those presented on Figure 7. These two curves are compared to the simulated outlet temperature obtained by taking the average of the four measured ground temperatures as the far-field temperature. As shown in this Figure, the prediction of the outlet temperature using the average ground temperature is not as good as the case where four ground temperatures are used. This is particularly true during the off-cycles where the simulated outlet temperature tends towards the average ground temperature (i.e. ≈ 10.4°C) which is about 3°C higher than the prevailing ground temperature at a depth of 1 m where the sensor is located. This highlights the need to take into account the variation of the ground temperature near the surface when simulating short boreholes.

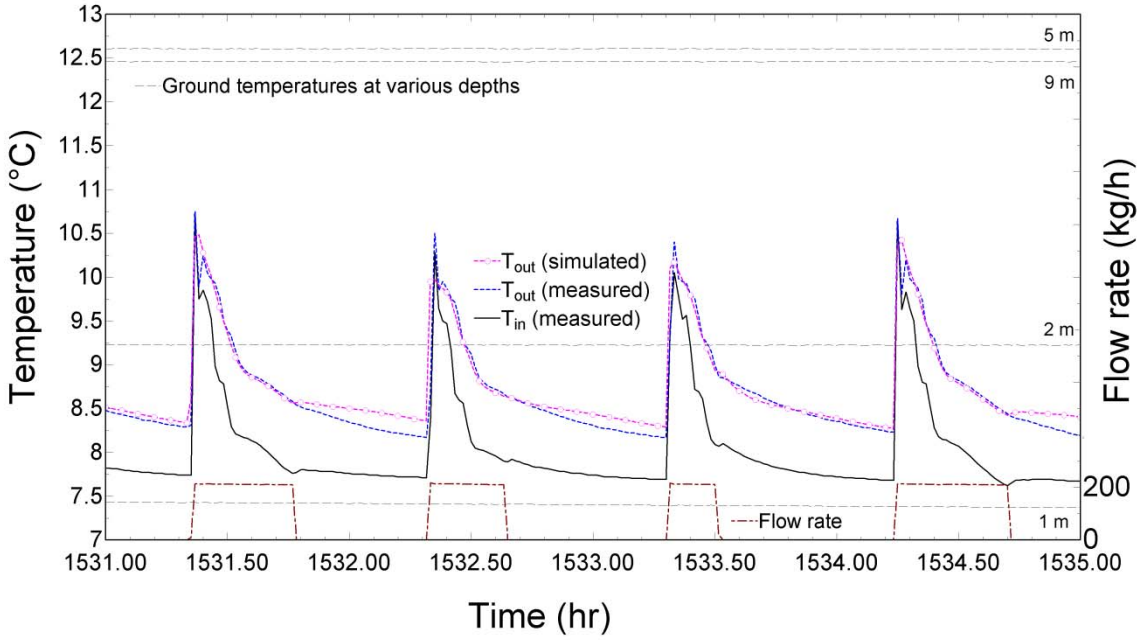

Figure 7: Comparison between simulated and measured outlet temperatures for borehole #4.

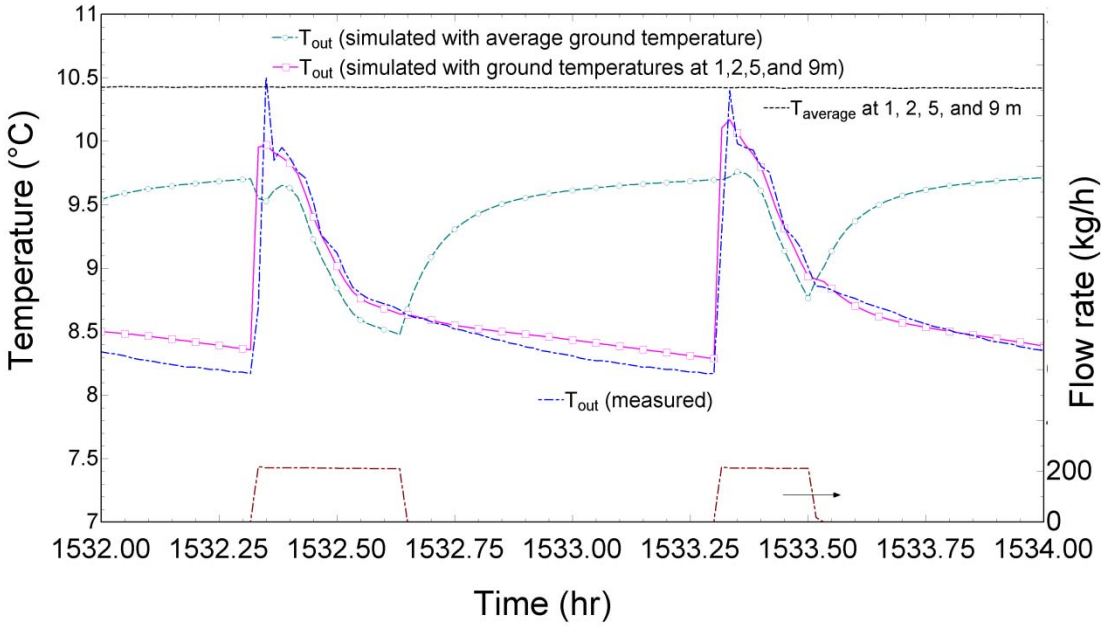

Figure 8: Impact of the choice of the far-field temperature on the simulated outlet temperatures for borehole #4

4.2 Entire bore field

Figures 9 shows comparisons between simulation and experimental results for the entire bore field in the middle of the heating season. Temperatures at the outlet of each row for a period of about 43 minutes with an on-cycle lasting 20 minutes (from $t \approx 0.16$ to ≈ 0.175 days) are shown. The measured temperature at the inlet of borehole #1 is also plotted (the other 3 inlet temperatures for each row are similar). This last curve shows that the inlet temperature decreases rapidly when the pump starts (shortly before $t = 0.16$ days) then it climbs back before decreasing again. This indicates that the fluid upstream of borehole #1 has pockets of fluid at different temperatures that are successively introduced at the initiation of the on-cycle. After $t = 0.165$ days, the inlet temperature is more or less constant at around 4°C. The four measured outlet temperatures of each row (i.e. outlet temperatures of boreholes #4, #5, #12, and #13) show a similar transient behavior at the beginning of the on-cycle. Then the temperatures decrease steadily before reaching a value of ≈ 8°C at the end of the on-cycle. These four outlet temperatures are close to each other indicating a good flow distribution in each row. The simulated outlet temperatures are obtained using the bore field model proposed earlier using as inputs the measured inlet temperatures and flow rates to each row. The far-field temperature was set to the value measured at 5 m, i.e. 11.7°C, for the time periods shown in Figure 9.

Just before the on-cycle, the simulated outlet temperatures are much higher than the measured values. This is because the far-field temperature is set at a value corresponding to a depth of 5 m while in reality the outlets are at a depth of 1 m thus facing much colder temperatures. However, when the on-cycle starts, the simulated outlet temperatures decrease rapidly to reach the measured value at around $t = 0.167$ days, after the fluid had travel the full distance in each row. The agreement between the measured and simulated values is good towards the end of the on-cycle indicating that the proposed bore field model is more than adequate to predict the behavior of such a bore field. The agreement between simulated and measured temperatures would probably be improved during the off-cycles if the ground temperature at 1 m were used.

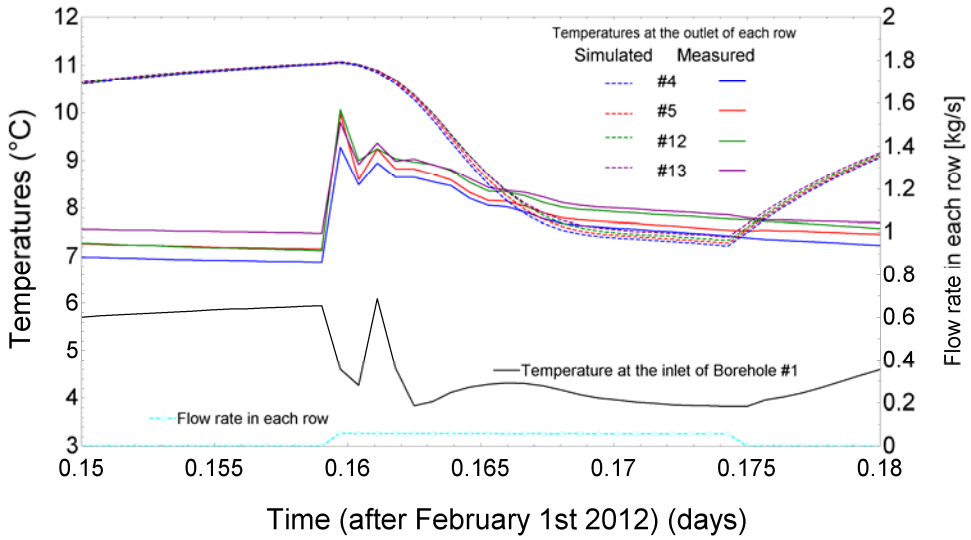

Figure 9: Temperatures at the outlet of each row (Boreholes #4, #5, #12, and #13) for a period of 0.03 days.

Figure 10 presents the results of energy balances performed on the entire bore field for seven on-cycles over a period of 0.25 days. The simulated values are higher that the measured values

in the beginning of each on-cycle. This is due to the overestimation of the outlet temperatures as shown in Figure 9. However, towards the end of each on-cycle, the agreement is much better with a difference of the order of 10% on an average heat extraction rate of ≈ 3.5 kW.

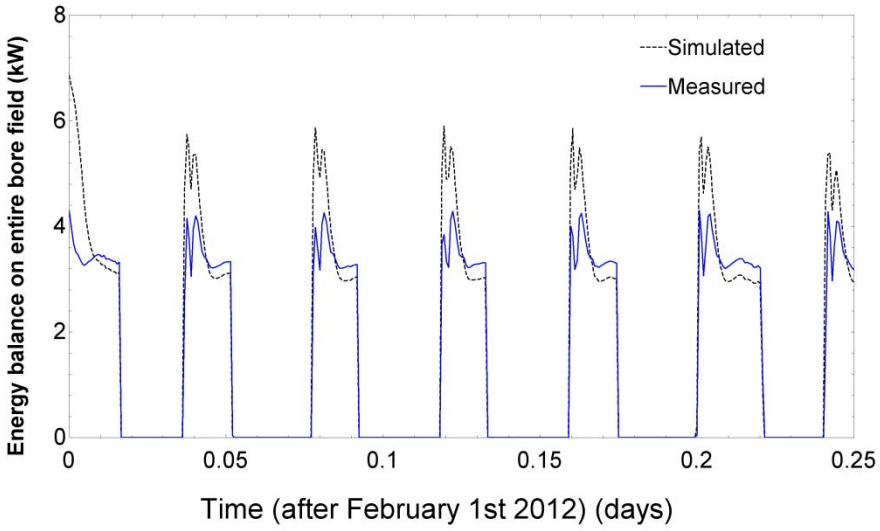

Figure 10: Simulated and measured energy balance for a period of 0.25 days

Finally, Figure 11 presents a graphical summary of the simulated inlet and outlet temperatures as well as the heat transfer rates per unit length for each borehole at t = 0.174 days (at the end of the on-cycle in Figure 9). These results show that there is a significant variation of the heat transfer rate per unit length in each row. For example, in the first row, the heat transfer rate per unit length varies from -24.16 W/m for the first borehole to -16.12 W/m for the last borehole. This is due to the fact that the inlet temperature changes from one borehole to the next.

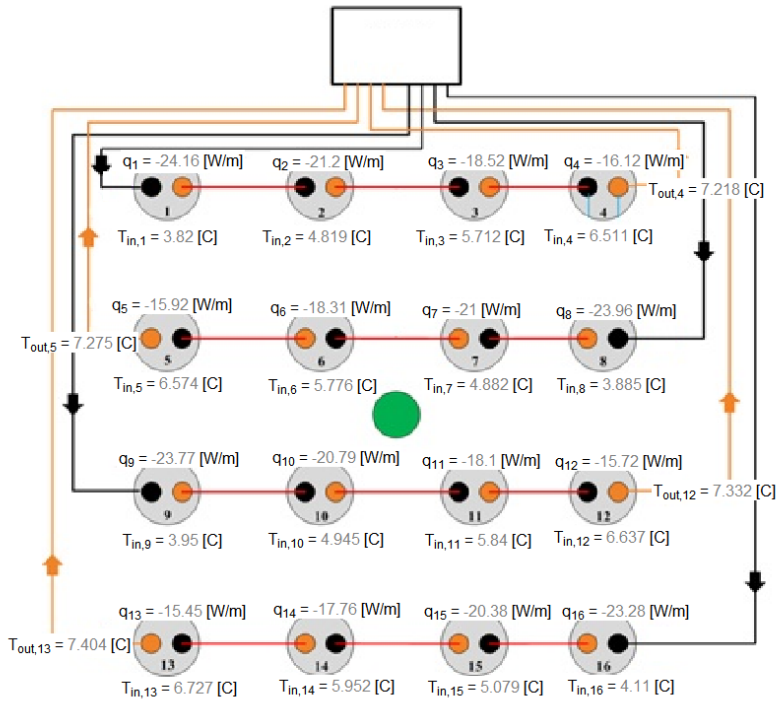

Figure 11: Simulation results showing inlet and outlet temperatures as well as heat transfer rate per unit length for all boreholes.

5 CONCLUSION

A methodology to model bore fields composed of short boreholes is proposed in the present study. First, a detailed single borehole model which includes borehole thermal capacity is introduced. Then, the entire bore field is modeled using analytical solutions to ground heat transfer and spatial and temporal superposition to predict the outlet fluid temperature from each borehole at each time step. The model is validated against experimental data obtained on a test facility composed of 16 short boreholes (9 m deep), with 4 rows of 4 boreholes in series. The single borehole model was compared with experimental results obtained with one borehole. The model was implemented in TRNSYS and simulations were performed over 1900 hours with a one-minute time step. Simulated and experimental results are in good agreement when the variation of the ground temperature with depth is taken into account. The use of an average temperature over the borehole length is inadequate especially during the off-cycles.

The model of the entire bore field was also compared to experimental data. It is shown that the model predictions of the outlet temperatures of each row are in close agreement with the experimental results during the latter part of on-cycles after the initial transient period. Simulated and measured heat extraction rates of the entire bore field agree within ± 10%. The results presented here highlight the importance of ground temperature variation in short boreholes modeling. Work is underway to refine the modeling tool to better represent these variations. The methodology will be extended to other bore field configurations with the objective of developing a validated design and simulation tool for bore fields composed of short boreholes.

6 REFERENCES

Bernier, M., P. Pinel, R. Labib and R. Paillot. 2004. “A Multiple Load Aggregation Algorithm for Annual Hourly Simulations of GCHP Systems”, HVAC&R, 10(4):471-488.

Cauret, O. and M. Bernier. 2009. “Experimental validation of an underground compact collector model”, Proceedings of Effstock 2009, 14-17 June, Stockholm, paper #44, 8 pages.

Cimmino, M. and M. Bernier. 2014. “A semi-analytical method to generate g-functions for geothermal bore fields”, *Int. J. Heat Mass Transfer*, 70(c):641-650.

Cimmino, M., M. Bernier and O. Cauret. 2013. “Validation d’un modèle pour la simulation de capteurs géothermiques compacts”, XIe Colloque Franco-Québécois, France, pp.277-282.

Claesson, J. and S. JAVED. 2011. “An analytical method to calculate borehole fluid temperatures for time-scales from minutes to decades”, *ASHRAE Transactions,* 117:279-288.

Eskilson, P. 1987. “Thermal analysis of heat extraction boreholes”, Ph.D. Thesis. University of Lund, Sweden, 264 pp.

Godefroy, V. and M. Bernier. 2014. “A simple model to account for thermal capacity in boreholes”. Accepted for presentation at the IEA 2014 Heat Pump conference.

Hellström, G., L. Mazzarella, and D. Pahud. 1996. “Duct ground storage model – TRNSYS version”, Department of Mathematical Physics, University of Lund, Sweden.

Rancourt-Ouimet, M. 2012. “Performance d'un champ de puits géothermiques verticaux peu profonds en boucle fermée”, M.A.Sc. thesis, Polytechnique Montréal.